EDITOR
F. RICHARD KEENE

Chirality in Supramolecular Assemblies

Causes and Consequences

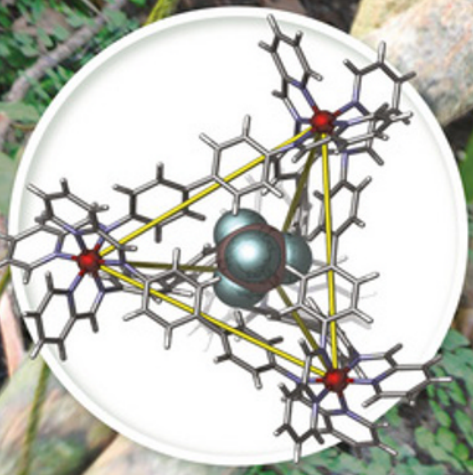

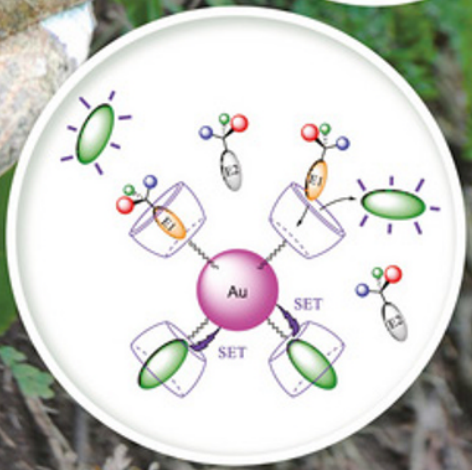

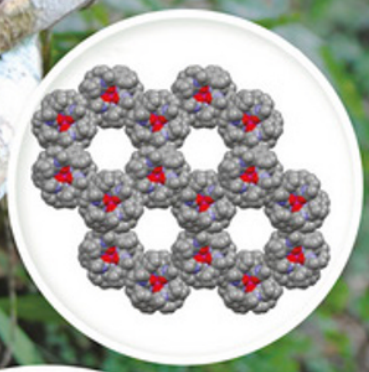

WILEY

Chirality in Supramolecular Assemblies

Chirality in Supramolecular Assemblies

Causes and Consequences

Edited by

F. RICHARD KEENE

Department of Chemistry,
School of Physical Sciences,
University of Adelaide, Australia

WILEY

This edition first published 2017

Registered Office
John Wiley & Sons, Ltd, The Atrium, Southern Gate, Chichester, West Sussex, PO19 8SQ, United Kingdom

Library of Congress Cataloging-in-Publication data applied for

A catalogue record for this book is available from the British Library.

ISBN: 9781118867341

Set in 10/12pt Times by SPi Global, Pondicherry, India

10 9 8 7 6 5 4 3 2 1

Contents

List of Contributors

David B. Amabilino, School of Chemistry, University of Nottingham, Nottingham, United Kingdom

Paul D. Beer, Inorganic Chemistry Laboratory, University of Oxford, Oxford, United Kingdom

Roger Bishop, School of Chemistry, The University of New South Wales, Sydney, Australia

Jean-Claude Chambron, Institut de Chimie Moléculaire de l'Université de Bourgogne, Dijon, France

Pedro Cintas, Departamento de Química Orgánica e Inorgánica, Facultad de Ciencias, Universidad de Extremadura, Badajoz, Spain

Jack K. Clegg, School of Chemistry and Molecular Biosciences, The University of Queensland, Brisbane, Australia

Steven De Feyter, Division of Molecular Imaging and Photonics, Department of Chemistry, KU Leuven-University of Leuven, Leuven, Belgium

Iris Destoop, Division of Molecular Imaging and Photonics, Department of Chemistry, KU Leuven-University of Leuven, Leuven, Belgium

Christopher J. Easton, Research School of Chemistry, Australian National University, Canberra, Australia

Nicholas H. Evans, Department of Chemistry, Lancaster University, Lancaster, United Kingdom

Daniel Fankhauser, Research School of Chemistry, Australian National University, Canberra, Australia

Philip A. Gale, Chemistry, University of Southampton, Southampton, United Kingdom

Declan P. Gavin, Department of Chemistry, Synthesis and Solid State Pharmaceutical Centre, University College Cork, Cork, Ireland

F. Richard Keene, Department of Chemistry, School of Physical Sciences, University of Adelaide, Adelaide, Australia

Jonathan A. Kitchen, Chemistry, University of Southampton, Southampton, United Kingdom

Edward G. Latter, Surface Science Research Centre and the Department of Chemistry, University of Liverpool, Liverpool, United Kingdom

Anita R. Maguire, School of Pharmacy and Department of Chemistry, Analytical and Biological Chemistry Research Facility, Synthesis and Solid State Pharmaceutical Centre, University College Cork, Cork, Ireland

John C. McMurtrie, School of Chemistry, Physics and Mechanical Engineering, Queensland University of Technology, Brisbane, Australia

Rasmita Raval, Surface Science Research Centre and the Department of Chemistry, University of Liverpool, Liverpool, United Kingdom

David R. Turner, School of Chemistry, Monash University, Clayton, Australia

Preface

The origins of what is now called *supramolecular chemistry* have been somewhat disparate, arising in part from studies of the chemistry of macrocycles (a development of naturally occurring analogues), spherands and carcerands, and cryptates . . . but the award of the 1987 Nobel Prize to Donald Cram, Charles Pedersen and Jean-Marie Lehn in many ways gave it a consolidated focus and led to its emergence as a field that retains vigorous and distinctly multidisciplinary activities. Supramolecular chemistry – defined by Lehn as "the chemistry of molecular assemblies and of the intermolecular bond" – deals with the organization of molecules into defined assemblies using noncovalent interactions, including weaker and reversible associations such as hydrogen bonds, π-π interactions, dispersion interactions, hydrophobic and solvophobic effects, and metal-ligand interactions. The aspect of stereochemistry within such chemical architectures, and in particular *chirality*, is of very special interest as it impacts on considerations of molecular recognition, the development of functional materials, the vexed question of homochirality, nanoscale effects of interactions at interfaces, biocatalysis and enzymatic catalysis, and applications in organic synthesis.

This book is intended to address the nature of the phenomenon of chirality in its broadest sense, noting the change in its nuances and subtlety in the progression from simple individual molecules to molecular assemblies, and to show the manifestations of chirality in the synthesis, properties, and applications of supramolecular systems, emphasizing their multidisciplinary importance.

The book is essentially divided in to four broad parts. The first constitutes an introduction to chirality: Chapter 1 develops the concept of chirality from rigid isolated molecules through to assemblies of molecules (in supramolecular entities), to topological chirality. Chapter 2 discusses chirogenesis and the phenomenon of homochirality (loss of parity) in the development of naturally occurring polymers (including nucleic acids and polypeptides) – and its consequences for the formation of artificial supramolecular

aggregates. Chapter 3 provides an overview of chiral aspects arising in the crystallization of small organic molecules – principles that are applicable to all classes of molecules, including supramolecular assemblies.

The second part is predominantly (but not exclusively) centered on metallosupramolecular chemistry. By the use of examples, Chapter 4 addresses the diversity of supramolecular assemblies – and in particular metallosupramolecular assemblies – and describes the complexity of chiral structures and their construction through self-assembly procedures. Chapter 5 describes the role of chirality in molecular recognition and host-guest systems. Chapter 6 develops the notion that unique characteristics can be built into supramolecular assemblies because of features of chirality – characteristics that can lead to functional properties of such materials. Chapter 7 addresses bulk homochiral solids formed using chiral reagents – either by direct incorporation, or by templating or induction, during synthesis. Chapter 8 considers the basic design principles that underpin the construction of metallosupramolecular polyhedra.

The third part is devoted to chirality at interfaces. Chapter 9 focuses on chirality expression and amplification at solution / solid-state interfaces, and applications such as heterogeneous catalysis and chiral separations. Chapter 10 addresses the initiation of chiral suprastructures on surfaces, and their modeling by high-resolution experimental methods and theoretical calculations.

The fourth part addresses chirality in organic hosts, and in biological / enzymatic systems: organic hosts are used in analytical chemistry to separate racemic guest mixtures or simply to distinguish enantiomers, and chiral hosts can function as catalysts in asymmetric reactions – Chapter 11 reviews particular features and applications of chiral organic host systems based primarily on cyclodextrins, calixarenes, and crown ethers in this regard. Chapter 12 stresses the enormous potential of microorganisms and enzymes as catalysts in asymmetric synthesis for controlling the stereochemical outcome of reactions, and discusses the use of whole cells and isolated enzymes as an attractive option for the chemical industry.

It is always understood that supramolecular chemistry is so diverse that one book cannot be totally equitable in its coverage of all aspects of the field. This book attempts to address some of the major aspects authoritatively and highlight important current thrusts. It will be useful to researchers working with chiral supramolecular assemblies, and will hopefully draw others with an existing interest in supramolecular systems to a further appreciation of the importance of chirality in the field, as seen through contributions of experts in their respective parts of that firmament.

F. Richard Keene
Adelaide, Australia

1

Principles of Molecular Chirality

Jean-Claude Chambron and F. Richard Keene

1.1 General Introduction

Chirality is probably one of the most significant topics in chemistry. The strong connection between chirality and symmetry has made it appealing from the mathematical and aesthetic viewpoints, and the recent interest in topologically chiral interlocked and knotted molecules has increased its intellectual attraction, raising the concept of a hierarchy in chirality [1]. The most fascinating aspect of chirality stems from the dynamic properties of molecules and supramolecular assemblies, rather than their static properties, because they are the cause of many intriguing and sometimes paradoxical issues. At the same time, dynamic chirality is also the most useful topic because of the numerous applications it underpins, from chiral recognition to molecular motors.

Historically, chirality is rooted into crystallography (the concept of hemiedry), and the first breakthrough into the field of molecular chirality was Louis Pasteur's hypothesis that the dissymmetry of a crystal was a consequence of dissymmetry at the molecular level [2]. The second milestone was the Le Bel and van't Hoff model of the tetrahedral carbon atom, which accounted for the chirality of the organic compounds known at that time, and several years later Werner was the first to study and provide evidence for the chirality of metal complexes. The discovery of organic molecules that did not owe their chirality to tetrahedral carbon atoms carrying four different substituents (e.g., allenes, biphenyls, cyclophanes), and of helical structures in nucleic acids and proteins, finally led Cahn, Ingold, and Prelog to establish a general system for the description of chiral structures. Since then, many novel chiral molecules have been reported, and most of them could be described in the frame of the CIP rules. The most notable developments in chirality in recent decades concern aspects of the generation and control of chirality: transfer by supramolecular

Chirality in Supramolecular Assemblies: Causes and Consequences, First Edition. Edited by F. Richard Keene.

interactions; chirality of molecular assemblies (chirality at the supramolecular level or "supramolecular chirality"); and finally, the concept of "topological chirality" brought forward by the development of interlocked and knotted molecules.

This chapter constitutes an introduction to molecular chirality from the rigid geometrical model to the topological model, but also from the isolated molecule to assemblies of molecules. As the first chapter in this book on the causes and consequences of chirality in supramolecular assemblies, it will, nevertheless, not cover all the aspects of chirality transfer – in particular those resulting from a covalent bond formation.

1.2 Geometrical Chirality

A chiral object is the one that does not coincide with its mirror image. The source object and its mirror image are called enantiomorphs. From the point of view of symmetry, enantiomorphic objects can have only rotation axes C_n, $n \geq 1$, as symmetry elements: they are either asymmetric (C_1) or dissymmetric (C_n, $n \neq 1$). There are many natural examples of enantiomorphic objects, the prototypical one being the human hand, the Greek word for which (χειρ) has been used to create the English word "chiral." Molecules are objects at the nanometer scale that are made of atoms connected by chemical bonds. If molecules are considered as rigid nanoscale objects, the definition given above can be very easily transposed to the molecular level, with the term "enantiomorph" being replaced by "enantiomer." However, molecules differ from macroscopic objects according to two criteria: (i) they are not rigid and can encompass a great variety of shapes called conformations, the distribution of which depends on time, temperature, and solvent; (ii) they are not usually handled as a single object, but as populations of very large number of individuals (~ Avogadro number). These two unique characteristics make the definition of molecular chirality not as simple as that of a rigid object (such as a quartz crystal), and therefore it needs further developments in order to be refined [2].

The object molecule can be described at different levels of complexity, which are represented by models [3, 4]. The chemical formula, which uses atomic symbols for the atoms and lines for the bonds (traditionally, dashed lines for the weakest bonds), is no more than what has been termed a molecular graph, a concept derived from mathematics that has been introduced and used fruitfully in various areas of chemistry, in particular in molecular topology (see section 1.3). The structural formula is more informative because it shows the spatial relationships between the atoms and the bonds, which can be, for example, probed by nOe effects in NMR spectroscopy. The most accomplished description of the molecule as a rigid object is the 3D representation resulting from an X-ray crystal structure analysis, as it gives the distances between the atoms (bond lengths), and the angles between bonds. This points to the fact that the image of the molecule we have depends on the observation technique – in particular its timescale, observation conditions such as temperature, but also the state of the observed molecule (solid, solution, gas) [5]. In fact, a large number of molecules, including chiral ones, can be described using the approximation of rigidity (i.e., a rigid model) because fluctuations of atom positions are averaged around a thermodynamic equilibrium value at the observation timescale. In that approximation, as pointed out by Mislow [4], the chirality of the molecule is the chirality of the model, which depends only on the atomic positions, so that in principle the bonds can be ignored. However, the

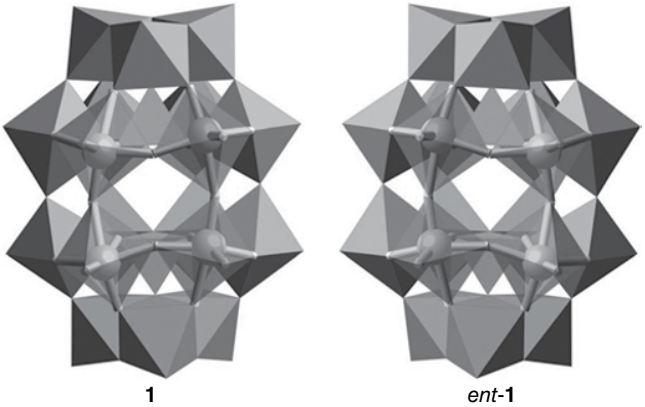

Figure 1.1 *The enantiomers of the chiral Keggin polyoxometallate α-$[P_2Mo_{18}O_{62}]^{6-}$* ***1****. The chirality of this molecule has a dynamic character, which allows the dynamic thermodynamic resolution of a given enantiomer of this hexaanion by interaction with enantiomerically pure cations*

presence of a bond between two atoms indicates that these atoms are closer to each other than if they were not bonded, so that, in practice the bond formalism is very useful for assessing, in a straightforward manner, the chirality of a rigid molecular model. This is the case where, for example, within two identical sets of atoms symmetry-related bonds have different lengths, leading to a distortion of the entire structure. Such an example of chirality due to alternating bond lengths is illustrated by the Keggin polyoxometallate α-$[P_2Mo_{18}O_{62}]^{6-}$ **1** of Figure 1.1 [6].

1.2.1 Origins and Description of Chirality within the Rigid Model Approximation

1.2.1.1 General Considerations

This section will deal with general considerations relating to the description and origins of chirality. Examples selected for their unique chirality properties will be then discussed in more detail in the following sections. Rigidly chiral molecules can only undergo rotations about bonds. They belong to one of the following point groups: (C_1, asymmetric), C_n, D_n, T, O, and I – the latter three being quite rare (see section 1.2.1.3) – which contain only proper symmetry axes as symmetry operations (Table 1.1). Molecular chirality concerns molecules or molecular assemblies featuring a 3D structure. The latter is determined by the interplay between molecular constitution, atom bonding geometry, and intramolecular and intermolecular interactions – including repulsions resulting from strain and steric hindrance. These factors then translate into arrangements of atoms that are either asymmetric (no symmetry element is present) or dissymmetric (with $C_{n>1}$ symmetry elements only) in the 3D space – the necessary but not sufficient (see below) criteria for chirality [2].

The conversion of a planar object into a 3D object can be achieved by either of two possible pathways. It is illustrated in Figure 1.2, starting from a rectangle as an example of a 2D object. Of course the rectangle, lying horizontally, is achiral (D_{2h} symmetry). In the first pathway let us take one of the points of the rectangle, for example its center, and pull

Table 1.1 *Symmetry elements of chiral point groups, the corresponding geometries they are generated from, and maximal symmetries*

Point group (achiral geometrical figure)	Symmetry elements	Symmetry properties
C_1 (general polyhedron)	None	Asymmetric
C_n, n≠1 (cone)	C_n	Dissymmetric
D_n, n≠1 (cylinder)	C_n, n × C_2	Dissymmetric
T (tetrahedron)	4 × C_3, 3 × C_2	Dissymmetric
O (octahedron and cube)	3 × C_4, 4 × C_3, 8 × C_2	Dissymmetric
I (icosahedron and dodecahedron)	6 × C_5, 10 × C_3, 15 × C_2	Dissymmetric

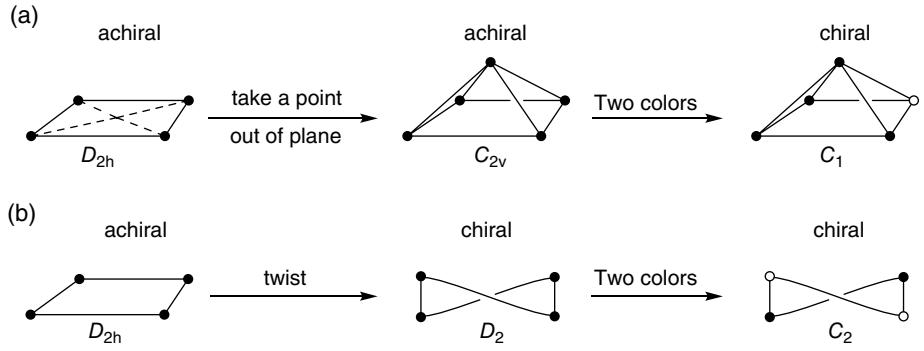

Figure 1.2 *Two pathways for the conversion of a planar object into a 3D object, exemplified by a rectangle. (a) Taking a point out of the plane of the rectangle generates an achiral C_{2v}-symmetric pyramid, of which the desymmetrization to a C_1-chiral object requires the use of two colored vertices (black and white). (b) Twisting converts the rectangle into a D_2-symmetric chiral object, the symmetry of which can be decreased to C_2 by coloring (black and white disks) of selected vertices*

it out of the plane along the vertical direction. This will generate a C_{2v}-symmetric pyramid. This achiral pyramid can be made chiral by changing its constitution – e.g. by coloring selected vertices: a minimum of two colors is required, as shown in Figure 1.2a, which produces an asymmetric (C_1) pyramid. The second pathway arises from a twist to the rectangle along its principal C_2 axis, which makes it a propeller with D_2 symmetry (Figure 1.2b). Hence, unlike the former case, the generation of chirality is simultaneous with the generation of a 3D object. Next, the symmetry is decreased to C_2 by color-differentiation of any two vertices out of the four. Of course, making three vertices of the same color would further decrease the symmetry of the propeller to C_1.

Stacks of an achiral planar object (such as an isosceles triangle, as shown in Figure 1.3) can produce an achiral D_{3h} symmetrical column (b), which upon a regular twist of the individual components is converted into a chiral wreathed column, either left- (a) or right- (c) handed.

In chemical vocabulary, the deformation applied to the rectangle of Figure 1.2a corresponds to a constitutional change as the rectangle (four vertices) has been changed to a

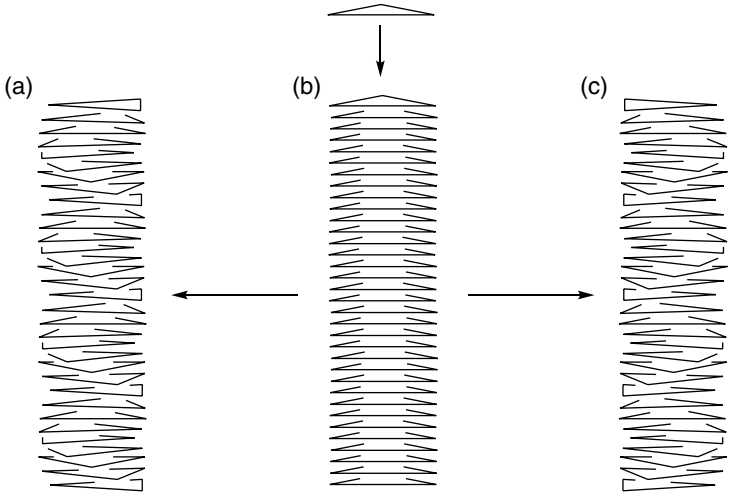

Figure 1.3 *Generating chirality by making (b) stacks of a planar triangular figure, followed by twisting of the resulting column either anticlockwise (a) or clockwise (c)*

pyramid (five vertices), whereas in the case of Figure 1.2b it corresponds to a conformational change as the twisted object has the same number of vertices and faces. Twisting may result from various mechanisms, such as rotations about bonds or variations in bond lengths – and in the case of molecular assemblies, from the generation of a curvature because of intermolecular attractions or repulsions.

The two basic processes of Figure 1.2 can be illustrated in the construction of the mirror-image molecular parallelepipeds $[Zn_2\text{-}\mathbf{2}]_4$ shown in Figure 1.4 by self-assembly of Zn(porphyrin) covalent dimers (*R*)-Zn_2-**2** and (*S*)-Zn_2-**2** driven by the Zn-pyridyl interaction [7]. The vertices of the cubes are occupied by Zn porphyrin (ZnPor) subunits, whereas four parallel edges are formed either by *meso* C–C single bonds or the *meso* C–(4-pyridyl)–ZnPor bond sequence. The bis(porphyrin) subunits are twisted by 90° with respect to each other, while each Zn^{2+} cation has a pyramidal N5 environment in the assembly.

The specification of chirality was formalized by Cahn, Ingold, and Prelog using (in the first instance) the "chirality model," which involves three stereogenic elements of chirality: the center, the axis, and the plane [8]. The chirality model of molecules is based on the tetrahedron, which is also the minimal 3D polyhedron [9]. In the first case (asymmetry, Figure 1.5) the perfect tetrahedron of T_d symmetry needs four different achiral vertices (A, B, C, and D) to be C_1 chiral (asymmetric constitution). Another possibility is to consider a tetrahedron of C_1 symmetry, in which all six edges have different lengths (asymmetric arrangement of the atoms). In practice, the asymmetric tetrahedron results both from asymmetric constitution and atom arrangement (Figure 1.5d).

In the second case (dissymmetry, Figure 1.6), elongation along one of the C_2 symmetry axes of the tetrahedron of Figure 1.5a decreases its symmetry to D_{2d}, and therefore only two different achiral substituents (A and B) are now needed to make it C_2-symmetric chiral. In addition, the D_{2d} elongated tetrahedron can also be made chiral without the need of substituents, by differentiating another pair of edges that are related by the main C_2 axis (z direction). This is done by compressing the tetrahedron of Figure 1.6a in the y direction,

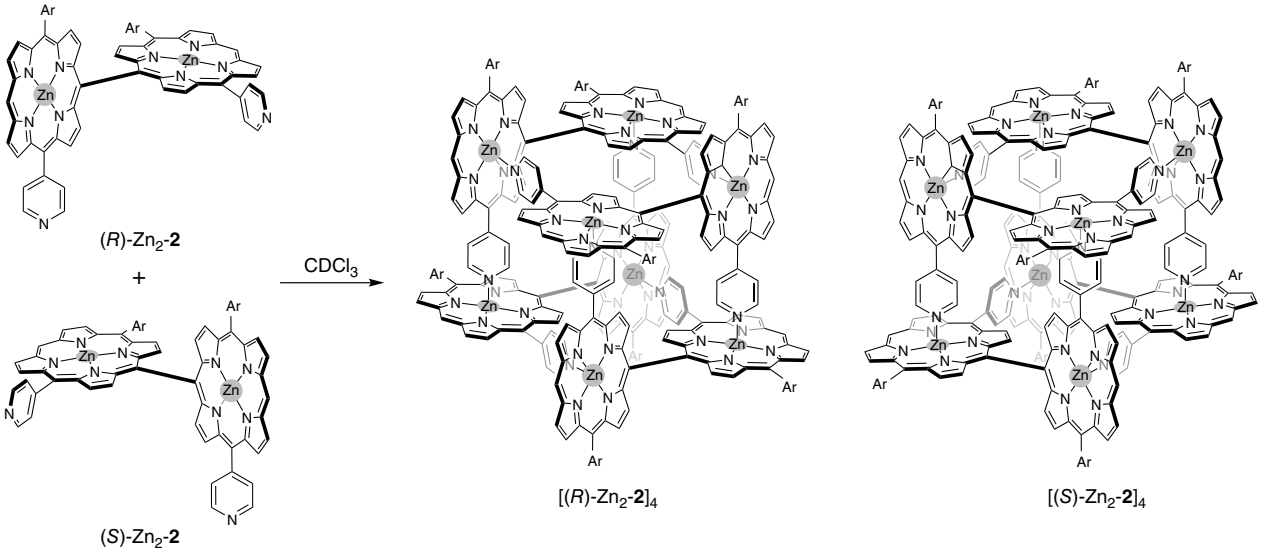

Figure 1.4 *Formation of homochiral assemblies [(R)-Zn_2-**2**]$_4$ and [(S)-Zn_2-**2**]$_4$ from twisted Zn(porphyrin) covalent dimers (R)-Zn_2-**2** and (S)-Zn_2-**2**, based on the Zn^{2+}-pyridyl interaction*

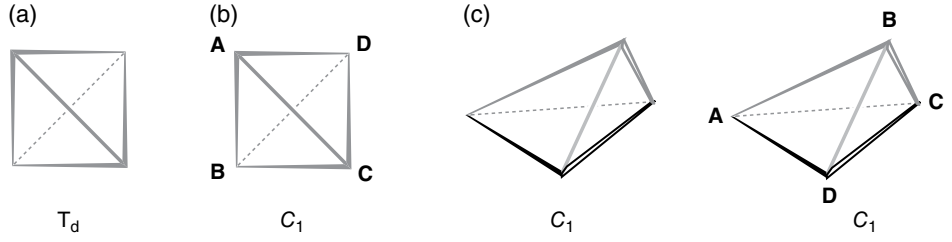

Figure 1.5 *Making the regular, T_d symmetric, tetrahedron (a) asymmetric: (b) by assigning the vertices four different labels; (c) by differentiating the lengths of all six edges using six different "colors"*

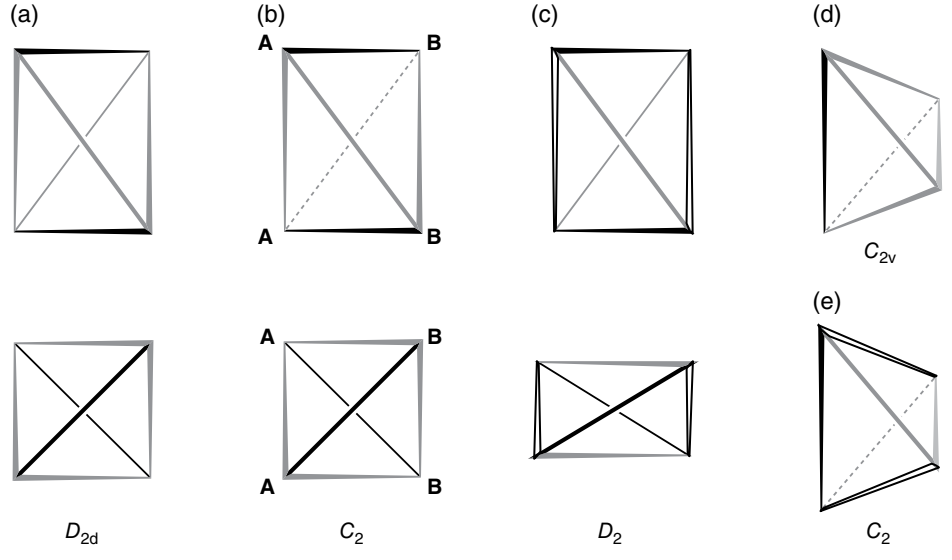

Figure 1.6 *Desymmetrization of the regular tetrahedron. (a) Elongation along one of the C_2 symmetry axes makes the two edges that are perpendicular to it (colored in black) different from the others. A view from the top is shown below the side view. (b) This D_{2d}-symmetric tetrahedron is made C_2-symmetric by labeling the four edges with two different labels, A and B. (c) It can be made D_2-symmetric by further coloring (in white) two edges that are symmetry related by the main C_2 axis. As shown in the top view below, this corresponds to a second elongation, along the C_2' axis. (d) The symmetry of tetrahedron (a) is further decreased to C_{2v} by differentiating a third edge (colored in light gray). (e) The latter is made C_2-chiral by coloring in white two edges that are related by the C_2 symmetry axis, leaving the two others in dark gray*

which removes its symmetry planes. The resulting tetrahedron (Figure 1.6c) is D_2-symmetric. Decreasing the symmetry of the D_{2d} tetrahedron further by moving symmetrically two vertices closer to each other as shown in Figure 1.6d, produces a C_{2v}-symmetric tetrahedron, which is made C_2-symmetric chiral by differentiating a pair of C_2 symmetry-related edges (Figure 1.6e).

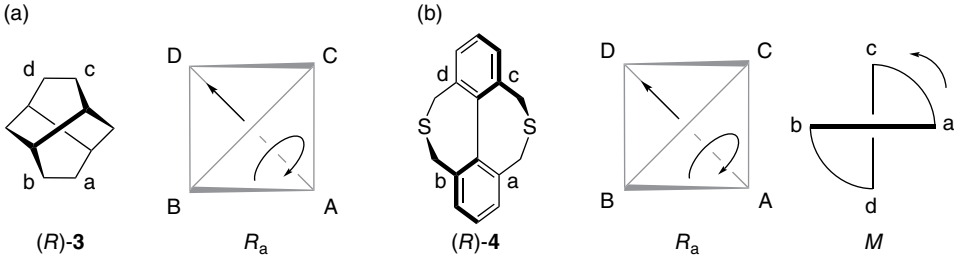

(*R*)-**3** R_a (*R*)-**4** R_a *M*

Figure 1.7 *Description of chirality using the chirality axis as stereogenic unit (a, b), and comparison with the description of chirality by identification of a twist (b). a) (+)-Twistane* ***3****. The chirality axis bisects [a, b] and [c, d]. b) A* D_2*-symmetric doubly bridged biphenyl* ***4****. The chirality axis is the biphenyl Ar-Ar bond. In both cases the positions of a and b are arbitrary, however the CIP rules govern those of c and d. Biphenyl (b) is also a molecular propeller, the conformation of which is* M

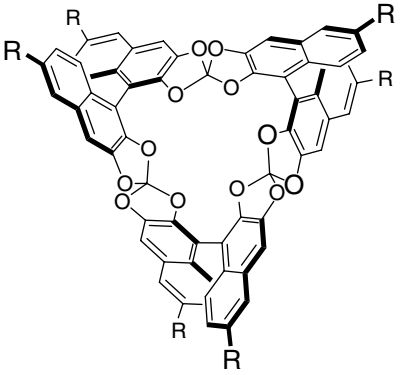

(*R*,*R*,*R*,*R*,*R*,*R*)-**5** (R = H or *n*Bu)

Figure 1.8 *The 3D triangular Janus cyclophane* ***5*** *is made by connecting three homochiral binaphthol-derived subunits by three carbon bridges. The configuration of all six chirality axes is* R

Figure 1.7 illustrates how two molecules, the 3D structures of which arise from different factors, are described using the same formalism (the chirality model) – in this particular case, the chiral axis. (+)-Twistane **3** (Figure 1.7a) owes its chirality to a highly symmetrical arrangement of sp^3 carbon atoms in space. The ansa-biphenyl **4** of Figure 1.7b is D_2-symmetric chiral due to strain-relieving twisting. Both molecules have the same configuration (R_a), which is obtained from the chirality model. In addition, the biphenyl can also be considered as a molecular propeller, and as its 3D structure is of conformational origin, it is best described using the *M*/*P* nomenclature. From the CIP rules, it is the *M* conformation that corresponds to the R_a configuration.

An additional illustration of the chirality axis is given in Figure 1.8, which shows a tris(spiroorthocarbonate) cyclophane (**5**) made in low yield by condensation of (*R*)-2,2′,3,3′-tetrahydroxy-1,1′-binaphthyl with dichlorodiphenoxymethane as the carbon source in refluxing toluene [10]. The resulting D_3-symmetric cyclophane has six chirality axes, three

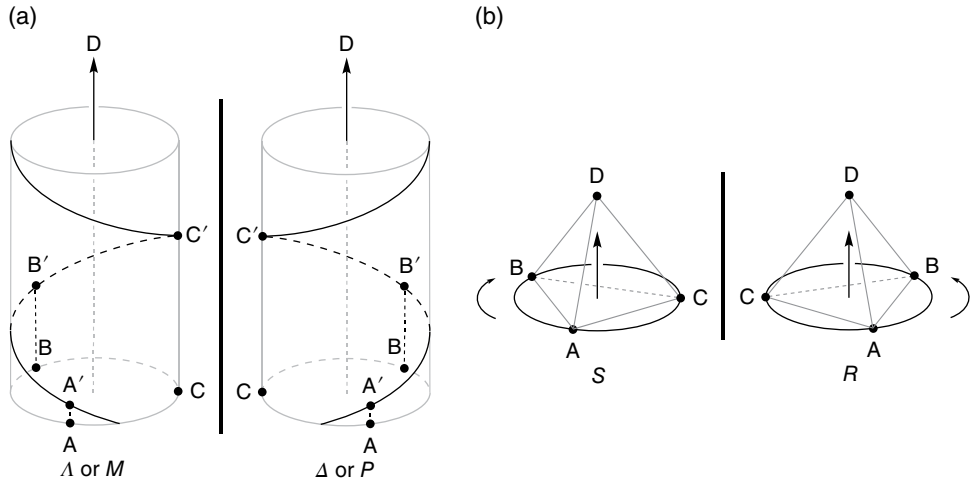

Figure 1.9 *Two different ways to define and orient the 3D space and the analogies between them. (a) Definition and orientation of the 3D space within the helicity model: generation of a helix and description of helical chirality using the Λ, Δ or* M, P *descriptors. (b) Chirality model: reduction of the stereogenic unit to a tetrahedron substituted with four different substituents (descriptors* S *and* R*). The vertical arrows are oriented towards the face from which the ABC plane must be seen. In (a) the D point has been sent to the infinite. Note that, when both models can be equally applied, there is no relationship between the helicity and chirality descriptors, except in the case of the biaryls, where* M *and* P *correspond respectively to* R *and* S

of conformational origin from the binaphthyl components, and three of configurational origin from the spiroorthocarbonate connections, which are interdependent. This molecule features two back-to-back aromatic concavities, which were shown by X-ray crystallography to be able to complex two C_{60} guests via multivalent π-π interactions.

The other model that was devised by Cahn, Ingold, and Prelog is the "helicity model," which proved subsequently to be extremely relevant in describing the chirality of a great variety of molecules and polymers, in spite of the fact that – at the time it was proposed – examples of helical nanoscale objects were rare [8]. From the mathematical viewpoint, a helix results from the combination of a rotation and a translation, and can be cylindrical (C_2 symmetry) or conical (C_1 symmetry). Once a helical structure is clearly identified, for example as a secondary structure, the sense of chirality is given by the helical path. If a clockwise rotation produces a translation away from the observer (following the sequence A′, B′, C′ in Figure 1.9a), the sense of chirality is *P* or *Δ*; if the same effect is produced by a counterclockwise rotation, the sense of chirality is *M* or *Λ*. Note that *P* and *M* descriptors generally apply to conformations and to the so-called secondary structures, and that the *Δ* and *Λ* descriptors are used for the configurations of transition metal complexes.

Natural macromolecular compounds such as DNA, polypeptides, and amylose, as well as synthetic examples such as polyacetylenes and polyisocyanates, can take up helical shapes [11]. This is also the case with molecular compounds like foldamers [12], helicenes [13], and helicates [14] (Figure 1.10). Larger structures encompass at least a full helix turn. By contrast, the smaller members of these families of molecules do not incorporate a 360° turn

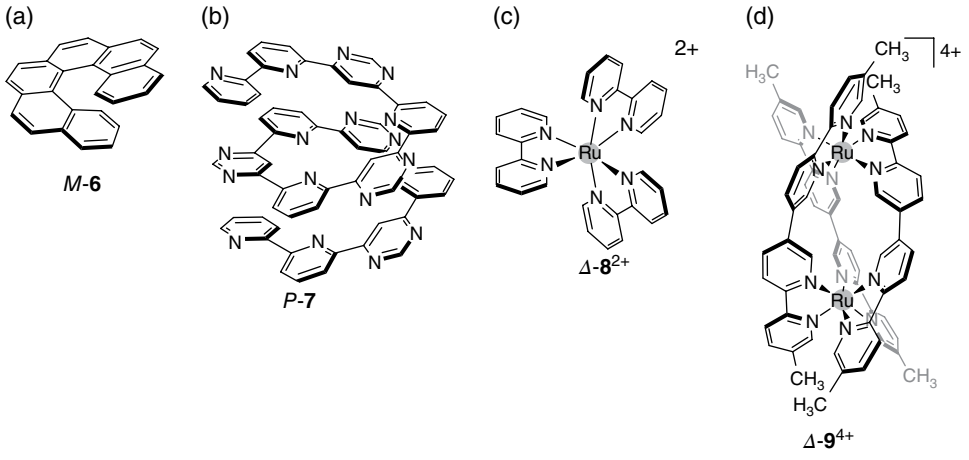

Figure 1.10 *Examples of helically chiral molecules and molecular propellers. (a) [6]Helicene* ***6****. (b) Foldamer* ***7*** *based on alternating pyridine and pyrimidine subunits. (c) The* $[Ru(bipy)_3]^{2+}$ *coordination complex (*$\mathbf{8}^{2+}$*), where bipy is 2,2′-bipyridyl, is a* C_3*-symmetric propeller. (d) Connecting two homochiral* $[Ru(bipy)_3]^{2+}$ *subunits through the positions 4 and 4′, respectively, of the bipy ligands produces a fragment of the triple helical dinuclear complex* $\mathbf{9}^{4+}$ *in which each quaterpyridine ligand has the same helical conformation*

and actually represent helical fragments: This is notably the case of the so-called molecular propellers [15] (Figure 1.10c), or of molecules that feature a simple twist (Figure 1.7b). Helicity can also manifest itself at the supramolecular level, for example in the case of helical stacks of achiral molecules. It is important to note at this stage that the formation of hierarchically organized chiral supramolecular structures can make the connection between nanoscopic and microscopic or macroscopic chirality (e.g., chiral molecular gels or chiral mesophases). The highest symmetry molecular propellers belong to the D_n symmetry point groups. Among D_n-symmetric propellers, those belonging to the D_2 symmetry point group are worth highlighting because they make the connection between the helicity model and the chirality model, as both models apply in that case (see Figure 1.7b).

As is the case for DNA, many helically chiral molecular compounds feature double or triple helices. This is particularly the situation for the helicates in which polychelate ligands take up helical conformations upon bridging at least two metal cations. This is illustrated in Figure 1.10d by the dinuclear Ru^{2+} complex of a quaterpyridine ligand ($\mathbf{9}^{2+}$) [16].

After this short overview of the origins and description of chirality we shall detail several examples that illustrate the two basic principles of formation of chiral structures in the 3D space shown in Figure 1.2 – that is, desymmetrization by constitution and desymmetrization by twisting.

1.2.1.2 Desymmetrization by Constitution

Figure 1.11 shows the grid-type tetranuclear metal-ligand assembly $[Os_2Fe_2(\mathbf{10})_4]^{8+}$ made from a "fused" bis(terpyridine)-like ligand (**10**) (in which two 2,2′-bipyridine moieties are bridged by a central pyrimidinyl fragment), and two different metal ions (Os^{2+} and Fe^{2+}),

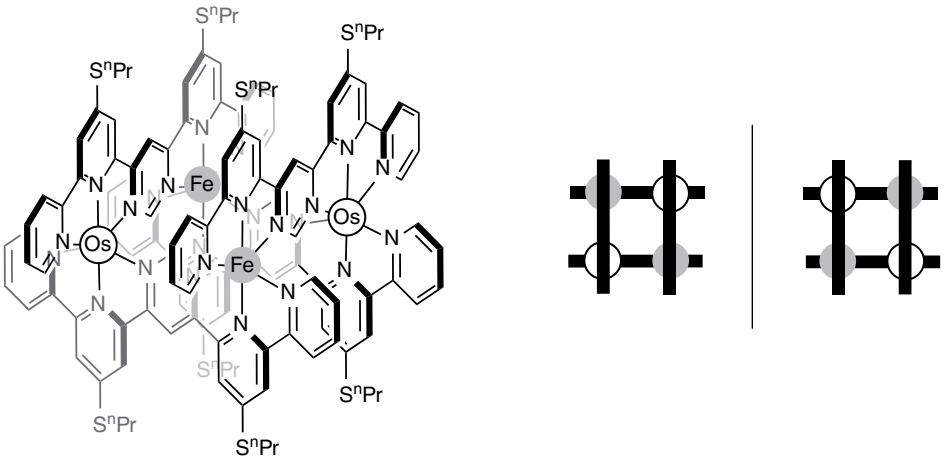

Figure 1.11 *The chirality of the grid-type tetranuclear complex $[Os_2Fe_2(\mathbf{10})_4]^{8+}$ of the "fused" bis(terpyridine)-like ligand* ***10***

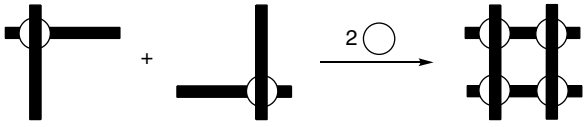

Figure 1.12 *The achiral D_{2h}-symmetric molecular grid is formed from two homochiral halves of mononuclear corner complexes with the bischelate ligands (black elongated rectangles) by addition of two metal cations that are identical to those involved in the starting homochiral complexes*

the pairs of identical metal centers being located on a diagonal [17]. This was done in a straightforward manner by introducing the metal centers in the order of increasing lability – reacting at first the di-chelate with NH_4OsCl_6 in 1 : 1 ratio, thus generating a corner-type chiral mononuclear complex, followed by the addition of $Fe(BF_4)_2$ (2 equivalents). Interestingly, the reaction proceeded stereoselectively to produce the chiral D_2-symmetric tetranuclear complex, as only corner-type precursors of the same handedness react with each other, excluding the formation of achiral *meso* C_{2v} assemblies. It is noteworthy that the tetra-homonuclear assembly represents a stereochemical curiosity, as it can be disconnected into two homochiral mononuclear di-chelate complex subunits. This illustrates the stereochemical paradox called "la coupe du roi" (Figure 1.12) [18].

Another remarkable case of desymmetrization by molecular constitution is offered by the higher order fullerenes. Fullerenes were unprecedented examples of molecules featuring a closed-shell structure. C_{60} itself has icosahedral I_h symmetry and is therefore achiral, but several higher order fullerenes such as $\mathbf{C}_{76}$, have been isolated and characterized. $\mathbf{C}_{76}$, which derives from C_{60} by incorporation of 16 additional C atoms, has D_2 symmetry, as shown by ^{13}C NMR (19 lines of equal intensity), and its chirality arises from its oblong,

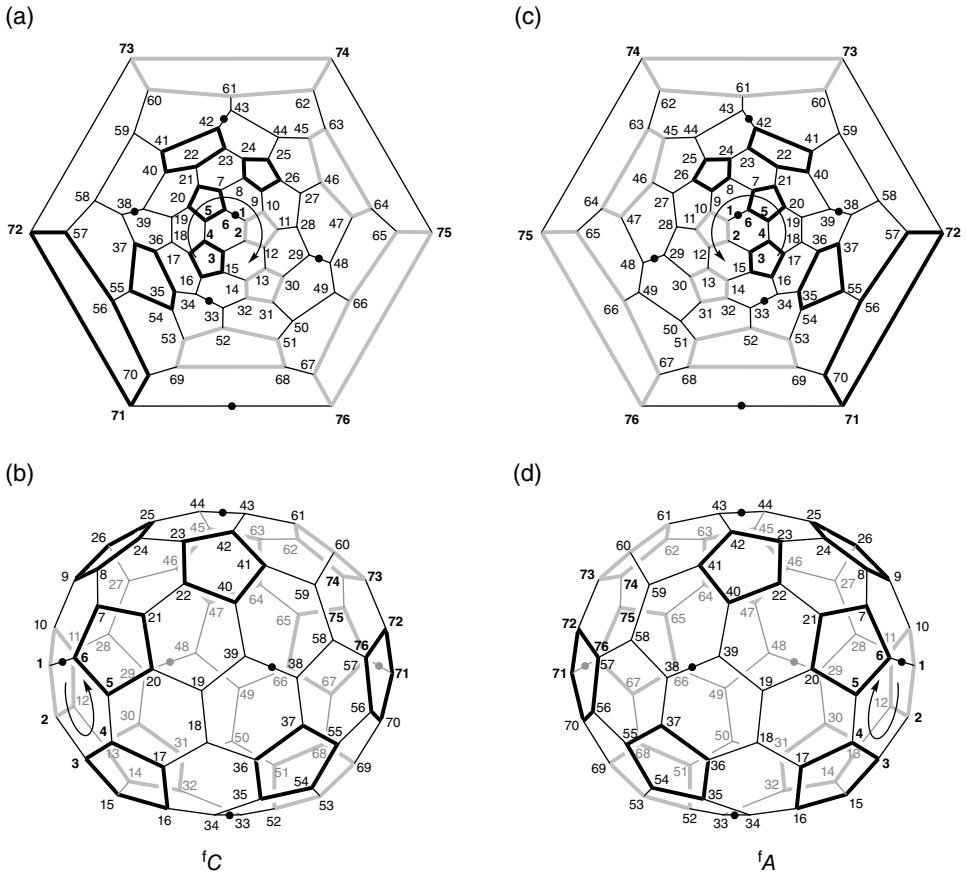

Figure 1.13 *Schlegel diagrams (a and c) and perspective representations (b and d) of the corresponding enantiomers of* $\mathbf{C}_{76}$*. The double bonds have been omitted for clarity. Five-membered rings have been highlighted in bold (black for the front ones, light gray for the rear ones in (b) and (d). The Schlegel diagram is obtained by opening the C71 to C76 six-membered ring and looking down the C1 to C6 analog (bold labels). The descriptor is* ^{f}C *if the C1 to C6 sequence is clockwise and* ^{f}A *if it is the opposite. The intersection of the three* C_2 *axes with the bonds have been materialized by the black dots: the vertical axis crosses C43–C44 and C33–C34, one horizontal axis crosses C1–C6 and C71–C76, and the other crosses C38–C39 and C29–C48*

helically twisted structure (Figures 1.13b to 1.13d) [19]. The enantiomers of $\mathbf{C}_{76}$ were resolved through the HPLC separation of the two diastereomers obtained by regioselective functionalization of $\mathbf{C}_{76}$ with an optically active malonate, followed by an electrochemical retro-Bingel reaction performed on each isolated diastereomer to release each optically pure $\mathbf{C}_{76}$. In principle, as all carbon atoms are pyramidalized, the configuration of the fullerene can be described by listing the absolute configuration (*R* or *S*) of each stereogenic center. The latter is obtained by developing the corresponding hierarchic directed graph which, however, is a cumbersome task.

Therefore a simplified procedure, which uses a single descriptor, has been developed which relies on the fact that the numbering schemes of fullerenes are helically chiral (Figures 1.13a to 1.13c), and can be used to differentiate between enantiomeric fullerenes. Whereas two isometric mirror-symmetric numbering schemes can be applied to an achiral parent fullerene such as C_{60}, a unique one is associable with a specific enantiomer of an inherently chiral carbon spheroid. Depending on whether the path traced from C(1) via C(2) to C(3) of this numbering is clockwise (C) or anticlockwise (A), the descriptors are defined as ^{f}C and ^{f}A. Figures 1.13a and 1.13c show the Schlegel diagrams of the enantiomers of $\mathbf{C}_{76}$ viewed through the opening of the six-membered C71–C72–C73–C74–C75–C76 cycle in the direction of its C1–C2–C3–C4–C5–C6 analog. The sense of the latter sequence (clockwise or anticlockwise) gives the chirality descriptor ^{f}C or ^{f}A. As $\mathbf{C}_{76}$ is D_2-symmetric, it has three C_2 symmetry axes that are orthogonal to each other.

Concave, bowl-shaped molecules represent a very important family of receptors and precursors of receptors that may display chirality [20]. Examples are resorcinarenes, calixarenes, cyclotribenzylenes and cyclotriveratrylenes, tribenzotriquinacenes [21], sumanenes [22], subphthalocyanines [23] and receptors built from these compounds – such as the cryptophanes made by dimerization of functionalized cyclotribenzylenes [24], or molecular capsules assembled by hydrogen bonding between urea-functionalized calix[4]arenes [25]. As concave molecules are nonplanar, they can be made chiral just by rim orientation. The simplest geometrical model of a concave molecule is a tetrahedron with an "empty" ABC face opposed to the D vertex [26]. Calix[4]arenes carrying at least two different substituents in the *para* positions of the phenol rings, or having even a single *meta* substituent, such as **11** (Figure 1.14a) [27], cryptophanes carrying two different substituents at the *meta* positions of the phenylene rings, such as **12** (Figure 1.14b) [24] – just to mention a few – are examples of concave molecules that owe their chirality to rim orientation. These compounds have been qualified as "inherently chiral," because their chirality (which does not depend on the presence of chiral substituents) is a property of the overall structure [26]. However, this expression may be misleading as bowl inversion, when it is possible, reverses the sense of chirality: therefore concave molecules are better described under the heading of conformational chirality [28]. The recommended descriptors to characterize these molecules are *P* and *M* [8]. Rim orientation of achiral concave molecules may also result from the concerted orientation of substituents, for example by a directed network of hydrogen bonding. The self-assembled molecular capsule $(\mathbf{13})_2$ of Figure 1.14c is obtained by Et_4N^+-templated head-to-head dimerization of two urea-substituted calix[4]arene (**13**) components [25].

Cyclodextrins are concave macrocyclic oligomers of *D*-glucose, and are therefore enantiomerically pure compounds. The recent development of efficient methods for the selective functionalization of their primary rim has led, in particular, to the synthesis of α-cyclodextrins carrying three different substituents [29]. Figure 1.15 shows an example in which the original primary alcohol functions have been replaced by $-PPh_2$, -OBn (Bn is CH_2Ph) and -Me groups that alternate twice, which imparts an orientation to the primary rim. Therefore, the modified cyclodextrin has two diastereomers **14a** and **14b**, because the chirality due to rim orientation is superposed on the chirality of the native cyclodextrin backbone. The resulting molecule can be considered a diphosphine ligand, and indeed it was used in the Tsuji–Trost allylation reaction. It was shown that opposite orientations of the primary rim led to opposite enantioselectivities, albeit rather low (30%), whereas the

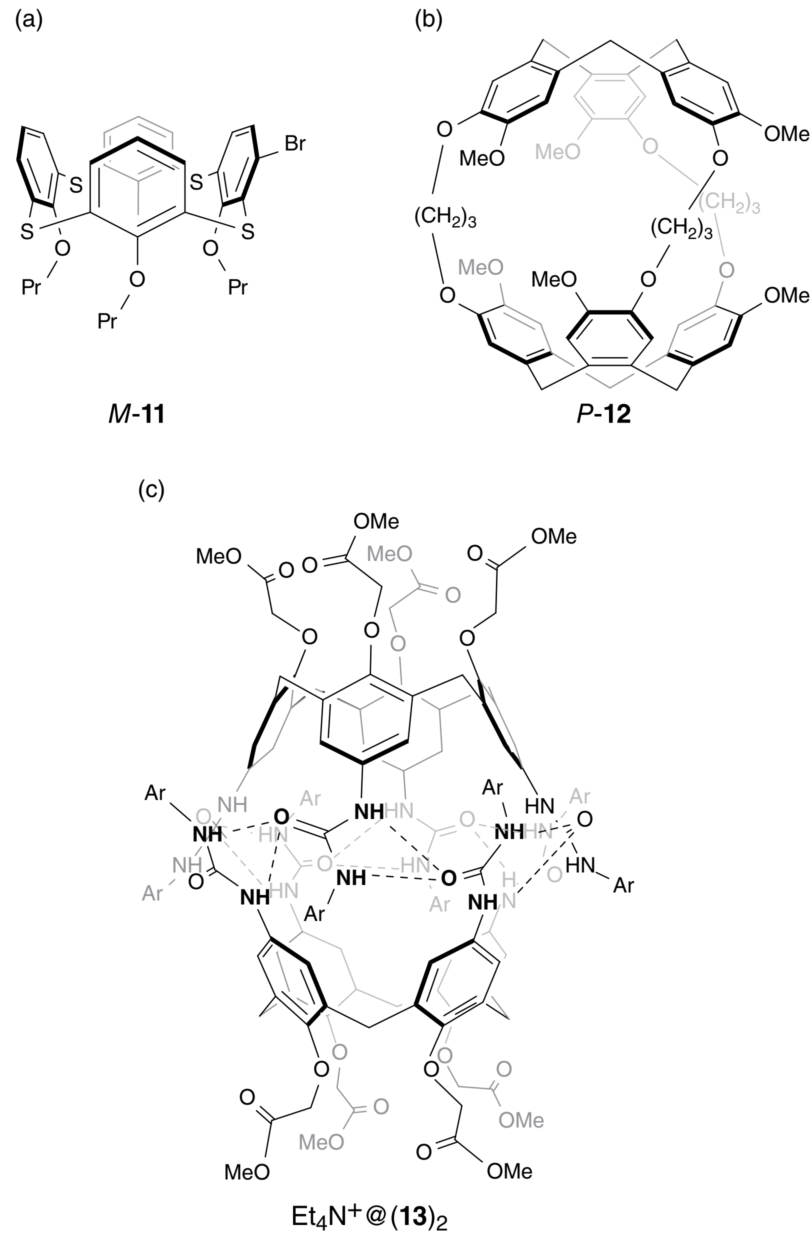

Figure 1.14 *Examples of concave chiral molecules. (a) One of the phenyl rings of thiacalix[4]arene **11** bears a bromine atom in the* meta *position, which destroys the* C_{4v} *symmetry of the parent compound, and makes the corresponding system asymmetric. The propyl groups prevent ring inversion at ambient temperature. (b) Cryptophane-A (**12**) in the chiral,* anti-*configuration* (P). *(c) A head-to-head calix[4]arene dimer* $(\mathbf{13})_2$ *via hydrogen bonding between arylurea substituents, that encapsulates* EtN^+ *(removed for clarity; Ar =* p-*tolyl). The methyl acetate substituents maintain the macrocycles in the cone conformation*